International Journal of Advanced Technology and Engineering Exploration, Vol 10(106)
ISSN (Print): 2394-5443 ISSN (Online): 2394-7454
http://dx.doi.org/10.19101/IJATEE.2023.10101018

Research Article

A comprehensive control strategy for power quality enhancement in railway power system

Deepak Kumar Goyal[1*] and Dinesh Birla[2]
Department of Electrical Engineering, Government Engineering College, Bharatpur, Rajasthan, India[1]
Department of Electrical Engineering, Rajasthan Technical University, Kota, Rajasthan, India[2]

Received: 06-January-2023; Revised: 15-September-2023; Accepted: 19-September-2023

Abstract
The selection of the correct traction transformer reduces power quality (PQ) issues and minimizes the high impact of electrified railway systems (ERS) on the electrical grid. In contrast to power systems, the use of Yd11 transformers in ERSs is less common but represents a more suitable solution. This article assesses the performance of the Yd11 transformer in a traction power substation (TPS) and establishes its superiority over Scott and V/V transformers. The evaluation and analysis are carried out based on factors such as system connectivity, PQ, and economic considerations. A railway PQ compensator (RPQC) serves as the primary compensator, with the TPS acting as an auxiliary compensator in the analysis, both under balanced and unbalanced conditions. Simulation results validate the accuracy of the theoretical analysis. The proposed control system utilizes a proportional-integral (PI) controller integrated with a type-2 fuzzy logic controller (Type-2 FLC) due to the fast and dynamic nature of traction loads. Carrier-based pulse width modulation (PWM) signals are employed to generate pulse signals for the full bridge RPQC switches. The success of the suggested control technique is demonstrated through simulation results for V/V, Scott transformers, and Yd11 transformers. The results clearly indicate that the Yd11 transformer achieved superior performance, with distortion levels of 1.57% and 1.17% at loads ç=0.5 and ç=0, respectively.

Keywords
Electrified railway system, Full bridge converter, Railway power quality compensator, Type-2 fuzzy logic controller, Yd11 transformer, Traction power substation.

1.Introduction
Generally, different power quality (PQ) issues in railway traction arise due to alternating current-direct current (AC-DC) and alternating current-alternating current (AC-AC) converters [1]. The two main PQ issues that affect railroad traction and incur penalties are power factor (PF) and harmonics. Additional neutral currents are drawn by an unbalanced load brought on by single-phase traction loads [2]. Therefore, it is crucial to research and find out the best PQ conditioners for the railway traction system to prevent the impacts of PQ concerns. An analysis is processed [3] to quantify the numerous PQ issues that exist in power grids. PQ issues lead to low efficiency and poor PF in the systems.

To avoid paying a price for having a low PF, resistors have been traditionally employed to balance the PF, whether physically-operated or through computer control [4]. Initially, passive filters, also known as self-tuned filters, are utilized in the system to keep the oscillations within the limits.

The filters' constant compensation, high size, and resonance are their main shortcomings. Due to the fluctuating and sharply rising traction loads, an adaptive approach known as active filters has been developed [5]. Recently, academicians have been concentrating on the compensation for neutral current, reactive power, load balancing, and distortions. Light railway traction converters and auxiliary supply systems have seen a tremendous growth recently [6]. In a traction circuit, the testing of inverting amplifier with proper voltage levels and harmonics is a crucial stage. Direct current-direct current (DC-DC) converters are becoming increasingly significant in hybrid automobiles [7].

*Author for correspondence

Now, the focus is on adding soft-switched DC-DC converters in traction conversions to boost efficiency. Softer switching methods such as zero voltage switching (ZVS)/zero current switching (ZCS) are employed in DC-DC converters having parallel and series resonances, respectively [8]. The ZVS/ZCS-based converters contain higher switching frequencies and switching losses, therefore, further research is required to overcome those issues. This study mainly focuses on ZVS, ZCS, enhanced three-element resonant circuits, and supplementary cells in DC-DC converters. Soft-switched and multi-level DC-DC converters continue to be commonly used converter topologies in some traction applications [9]. This is made possible by the device's effective power conversion, low component count, cost-effective design, and strong transient responsiveness. However, a DC-DC converter is not a very sought after in response to the urban transportation dilemma because of leakage inductance in the linked inductor [10].

Traditional elements have already been used in a number of traction converters. The present already developed power converters make use of conventional circuits with insulated gate bipolar transistor (IGBT)-powered DC link voltages. ZVS or Z conditions are used by most soft-switched DC-DC converters to function. To lower overall switching losses and lessen voltage and current strains, new converter should be assessed. The advantages of the suggested converter over the ZCS and ZVS ones are enormous [11]. The main drawback of ZVS DC-DC converter was that the circuits are getting complex when the switch strains get turned on automatically [12].

With a focus on electro-magnetic interference (EMI) mitigation, voltage dips, and arcing difficulties, the next-generation electric railway power systems (ERPSs) are adopted, that are based on autotransformer-based 2.25 kilo-volt amperes (kVA) systems. In the literature, many combinations of passive and active compensating solutions were suggested to address the PQ issues linked to ERPSs. A lot of research is being done right now on upgrading outdated systems with sophisticated co-phase ERPSs based on power electronics (PE). Because the voltage source converters (VSCs) regulate the output voltage and currents to match the desired PQ [13], these ERPSs are known as “green types”. Several researchers have examined several PQ indicators in particular ERPSs during the past few years.

Harmonic issues in ERPSs are thoroughly being examined in a number of studies. A systematic study and methodology that tackles entire PQ events and categorizes them according to types of ERPS is still lacking, nonetheless. Additionally, the ERPS lacks an inclusive and all-encompassing resource, in contrast to power systems, for which numerous standards and resources are being produced [14]. By this, the ambiguity and complexity of PQ analysis in ERPSs was emphasized. A load with a high-power rating that changes dynamically is the electric train traction system. Additionally, PE converter used in this system results in issues with PQ including harmonic distortion, the sequence of current, voltage unbalance, voltage fluctuation, etc. The upstream power supply is impacted by this; hence compensation is required. In the meantime, choosing an appropriate approach to address PQ concerns requires thorough understanding and identification of the primary sources, occurrence environment, influencing factors, and features. Due to the aforementioned flaws, this work provides a thorough explanation and classification of PQ indexes and distortions along with a quick overview of different ERPS configurations and categories of reported PQ occurrences in literature based on each type of ERPS [15]. Therefore, to overcome the above-stated issues, numerous PQ issues and the transformer types are explored in this study. It primarily offers solutions for harmonic distortion and PF correction utilising a type-2 fuzzy approach. At the point of common coupling, studies are conducted both with and without improvement strategies. The findings show that the PF and overall harmonic distortion in the feeding bus have decreased by using proposed control technique. Currently, the design of many locomotives includes thyristor or diode converters that significantly lower the PF.

The following is a list of the study’s main contributions to overcome the above-stated issues:

- A new control method for railway PQ compensator (RPQC) systems is put forth in this study and is applied to various TPS transformer types.
- The current control system uses a regressive self-tuning proportional integral (PI) controller that is designed on type-2 fuzzy logic controller (Type-2 FLC) for quick dynamic response of traction loads.
- The output parameters are combined with carrier-based pulse width modulation (PWM) pulses to create signals for full bridge RPQC switches which account for distortions and reactive power in loads.

The structure of this research is mentioned as follows; Section 2 defines the existing works based on PQ in railway traction systems. Section 3 explains the process of the proposed full bridge converter (FBC) process and the Yd11 transformer control. Section 4 demonstrates the result analysis of the proposed system design. Section 5 provides the discussion and the limitations. Finally, section 6 states the conclusion part.

2.Literature review

To improve the traction system PQ and decrease control evaluation and process cost, Arabahmadi et al. [16] proposed a static volt ampere reactive compensator (SVC) incorporated railway power conditioner (RPC). Dual $1-\varphi$ voltage sources associated with the 2 feeder sectors through a $3-\varphi$V/V transformer served as the public grid's representation. The reactive power produced by the main compensator was decreased once the SVC was turned on or connected again to the traction supply, and the reactive power was completely balanced by the SVC. The device lacked in certain useful components; hence additional hardware was required for surge impedance correction.

The half-bridge-converter-based RPC (HB-RPC) was proposed by Amira et al. [17] to address the problem of PQ in electrified trains. The PI and genetic algorithm (GA) procedures were exploited to eliminate condenser voltage errors while retaining typical HB-RPC operation. Excessive reactive power from the traction was eliminated, due to the operation of HB-RPC. However, the result analysis demonstrated that the transformer connection had a similar impact on the control source.

To solve the problem of grid-side unbalancing, Goyal and Birla [18] discussed the various traction and impedance matching transformers. By using the star-delta traction transformer, the system was simulated in MATLAB, and results for both open-loop and closed-loop structures were produced. Without using an auxiliary transformer, the YD traction transformer and FBC helped to resolve the traction system's PQ.
The full-bridge five-branch modular multilevel converter (FB5B-MMC) was projected by Lei et al. [19] to assess its potential use for comprehensive PQ control of co-phase railway power system (RPS) in less-than-ideal operating conditions. The variable design phase of RC was highly efficient in performing phase compensation without sacrificing control stability over parameter variation and unpredictability. Harmonic current components of seventh and ninth orders were noted to be substantially worse.

A FB5B-MMC was recommended by Lei et al. [20] for the regulation of PQ in co-phase RPS with penetration of significant nonlinear inductive traction loads. This optimized scheme had far more evenly distributed branch current and losses throughout the 2φ-units of the FB5B-MMC, and had significantly higher overall branch capacity and power loss than scheme 2. Certain residual harmonics were present in the grid currents even after the rectification mechanism was activated, because of the transformers' nonlinear magnetization characteristics. According to Li and Shi [21], modular multilevel converter type RPC (MMC-RPC) equipment was used to control the PQ, reactive power and negative sequence module of railway traction system. The MMC-RPC with adaptive virtual synchronous generator (VSG) regulation was more stable in an event of a rapid variation in traction load. Here, an adaptive differential flatness control (DFC) was able to handle the active power balancing, compensation of reactive power, and suppression of negative sequence current (NSC). The VSG's tiny signal model showed that the system was stable when the control parameters were within the specific range, but this was challenging to achieve because of the variability in the operating conditions.

Wang et al. [22] developed the emergency power supply designed for photo-voltaic (PV) and battery accessible railway traction power supply system. The signal contained disturbance of a particular frequency during the steady-state of the system and used a Fourier transform to progress three ports of PV-battery locomotive network towards the inverter to connect the DC port. Applications of PV and battery emergency traction locomotives were not widely explored. Also, an extra investigation was required to discover the connection between PV and battery to protect the circuit.

Li and Shi [23] introduced MMC-RPC with distributed super-capacitor (SC) energy storage (ES) scheme. An ES scheme was adopted in which SCs were utilized as units of ES and linked through non-isolated DC/DC converter. Difficulties in the power value were solved by RPC which used back-to-back two-level voltage sourced converters, but at the same time it caused a huge number of harmonics. Current compensation (CC) method was adopted to control the balanced energy in the MMC-RPC system, but preservation of stability in system frequency was

complicated when the traction change was caused by lack of inertial support.

Lai et al. [24] presented a power transfer device that was integrated into a super capacitor to solve the PQ issue and low utilization rate of regenerative braked energy, in double-modes traction system. A hierarchical control approach which contained a converter control layer and energy management layer, was developed for quick and precise control performance. The PQ has not improved the PQ because there were some hot spots present inside the electrified railway.

Tang et al. [25] introduced the homogeneous method for traction power supply system based on wired transformers and multilevel modular converter. The suggested converter developed to solve the quality of electrical power supply issues and negative power locomotives connected with railways. However, the electric locomotive was unable to balance compensation with the locomotive power without using the compensator.

Suslov et al. [26] developed the electromagnetic field induced by compacted over headed lined (COHL) feed traction substation of mainline railroads. A system with railroads enabled the efficiency and application of COHLs for the traction substations. The concentric of conductors had performed to reduce the strength of electric field because the design were quite complex and entailed with higher constructed cost.

Suslov et al. [27] developed a digital model for flow analysis of railway power supply systems (RPSS) equipped with distributed generation (DG) units based on renewable energy resource. This model performed the technique of modelling in the phase reference frame. This model followed the following features such as system-wide consistency and it access the modelling power flows in a way that carried into the account properties. This model minimized the power supply cost, imbalanced data but this model had a high computational complexity.

Kampczyk and Rombalska [28] developed a geometric state of railway tracks which was sustained and developed with electric traction system. The suggested process was extremely beneficiated the scientific research and integrated into various methods which were applied of industry. The recommended method determined the meaningful and matched patterns with the presented data. However, the maintenance through the environment influenced the cost as high.

Fedele et al. [29] presented the neutral point clamped (NPC)-based multi-source inverters (MSI) for multimode DC rail traction systems. An onboard storage device designed in MSI-based architecture was processed. A theoretical analysis was exposed that control of dc currents was affected by an essential output power. After that, the reduced number of powers converters validated the both simulation and experimentation extensive on laboratory test bench standards. Each traction motor contains a switched ripples which was resolved by the motor induction winding. Even though, the ripple was appeared once again in the dc sourced current.

Riabov et al. [30] presented a mathematical model for train a movement on a section of the track at the manoeuvring. An energy model was changed the procedures in the traction electric drive, which utilized to perform the traction operation, while a train moves on a track section. With mathematical modelling, the energy estimation during movement on a track section was performed by all connected and certainly disconnected electric motors. However, this process consumed a much time and also had the computational complexity.

Kapoor et al. [31] analyzed the issue of distribution current in electric railway traction systems. The analytical expression displays specific loss to determine to main task of this analysis. Electric traction systems were among the largest consumers of electric power because it could be utilized economically to reduce the power losses and increase the efficiency. The prototypes were generally utilized for smaller-scale experimental setup, built to compute traction returned current, to simulate properly the possible dynamics and local conditions that hundreds of kilometres of traction current system have in real life.

Numerous studies have been proposed over the past several years to look into various PQ in a certain providing topology. Different PQ phenomena have been seen as a result of variations in the ERPS supply structure and different types of locomotives. This flexibility and growth have forced ERPS to deal with a variety of interactive interfaces, dependability and PQ issues. Additionally, the ambiguity and complexity of this issue have been heightened by the absence of standards specifically devoted to ERPS. This work proposes a thorough review of PQ

distortions and phenomena in various ERPS settings to offers a systematic classification. To reduce harmonics produced in traction power supply technique and remove NSC, Type-2 FLC was proposed.

3.Methods

This study provides a new modulation technique for RPC systems that improves the system efficiency by compensating for the NSC. The current strategy (Type-2 FLC) has a significant capacity for reducing RPQC rated power, also meeting the requirements of the prior control techniques. The RPC switch active and reactive powers from one source to the next and is completely made up of bridge converters with a similar DC-link capacitor that is mounted at the secondary winding of the traction power substation (TPS) [32]. In other terms, one converter serves as an inverter and introduces the active/reactive power into it, while the other converter operates as a rectifier and absorbs the whole power. The configuration of RPC in a TPS is demonstrated in *Figure 1* [33].

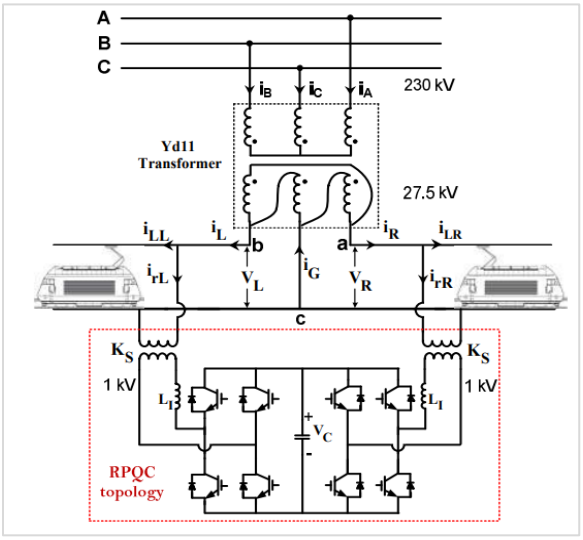

Figure 1 TPS configuration with RPC

To get around the 2-phase system issue, power is transported among two traction substations, via distribution lines operating in the same phase. The co-phase system reduces the costs while increasing the effectiveness of the traction system. PQ of the traction system is significantly impacted by low system voltage and high-power loss which decreases the effectiveness of the locomotive. A traction transformer is the only component in the system that functions as a connecter between a 3-phase supply and a 1-phase load. *Figure 2* depicts an example of a co-phase traction system [34].

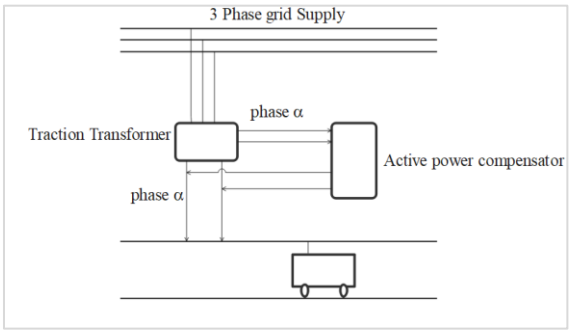

Figure 2 Co-phase modeling of traction systems

Electric railways experience unbalanced currents as a consequence of the motor's varied speed and changing load conditions. A FBC is exploited in combination with a Yd11 transformer to eliminate the unbalanced current [35].

There are numerous transformer types exploited in co-phase traction systems including:

- Yd11
- Scott
- Leblanc
- Impedance Matching

The Yd11 specifically changes the external grid's 3-phase feed to 1-phase [36]. Whenever the phase is linked to the load, the phase from the transformer acts as the active power compensator. A modulator is an AC-DC-AC converter that divides the load current by the voltage value, to produce the compensation for fundamental power components.

3.1Analysis of Yd11transformer

The Yd11 configuration is demonstrated in *Figure 3.*

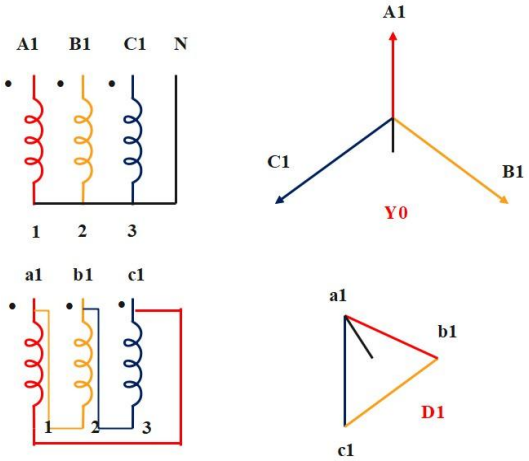

Figure 3 Yd11 transformer configuration

The load balance ratio is expressed to compute compensation voltages and currents that are represented in Equation 1 as follows:

$$\zeta = \frac{|I_{light-load\ section}|}{|I_{heavy-load\ section}|} \quad (1)$$

Voltage at primary windings is measured as Equation 2:

$$\begin{cases} V_A = \dot{V}e^{\iota 0} \\ \dot{V}_B = Ve^{\iota\frac{4\pi}{3}} \\ V_C = \dot{V}e^{\iota\frac{2\pi}{3}} \end{cases} \quad (2)$$

Consequently, secondary windings are stated as Equation 3:

$$\begin{cases} V_R = V_{\propto} = \frac{\dot{V}_{AC}}{a} = \frac{\sqrt{3}}{a}Ve^{i0} \\ \dot{V}_L = \dot{V}_{bc} = \frac{\dot{V}_{BC}}{a} = \frac{\sqrt{3}}{a}Ve^{-i\frac{\pi}{3}} \end{cases} \quad (3)$$

The currents at every segment are estimated in Equation 4 and Equation 5, taking into account PF near 1 and disregarding harmonics:

$$\begin{cases} \dot{V}_R = \dot{V}_{\propto} = \frac{\dot{V}_{AC}}{a} = \frac{\sqrt{3}}{a}Ve^{i\,0} \\ \dot{V}_L = \dot{V}_{bc} = \frac{\dot{V}_{BC}}{a} = \frac{\sqrt{3}}{a}\,V\,e^{-i\frac{\pi}{3}} \end{cases} \quad (4)$$

$$\begin{cases} i_A = \frac{i_R}{a} = \frac{Ie^{i0}}{a} \\ i_B = \frac{i_L}{a} = \frac{\zeta I e^{-i\frac{\pi}{3}}}{a} \\ i_C = -(i_A + i_B) = -(\frac{Ie^{i\,0}}{a} + \frac{\zeta I\, e^{-i\frac{\pi}{3}}}{a}) \end{cases} \quad (5)$$

As observed in Equation 5, the current amplitudes of two portions (Phase A & B) are out of balance since the primary currents remain asymmetrical. Phase A current is 30° behind Phase A voltage, and Phase B current is 30° ahead of Phase B voltage.

Secondary currents are imbalanced in amplitude when phase modelling of voltages and currents without compensation is taken into consideration which is expressed in Equation 6 and Equation 7:

$$\Delta i = |i_R| - |i_L| = I\,(1-\zeta) \quad (6)$$

$$\begin{cases} i_{\dot{R}} = i_R - \frac{\Delta i}{2}e^{i\delta} \\ i_{\dot{L}} = i_L + \frac{\Delta i}{2}e^{i\gamma} \end{cases} \quad (7)$$

δ and γ are phases of secondary currents. These currents are denoted as Equation 8:

$$\begin{cases} i_{qr} = tg\ 30° \times \frac{i_{\dot{R}}}{a}e^{i\frac{\pi}{2}} \\ i_{ql} = tg\ 30° \times \frac{i_{\dot{L}}}{a}e^{-i\frac{\pi}{2}} \end{cases} \quad (8)$$

By moving reactive power, these reactive currents are introduced. Therefore, the primary side three-phase currents are computed as Equation 9:

$$\begin{cases} i_A^{"} = i_A' + i_{qr} \\ i_B^{"} = i_B' + i_{ql} \\ i_C^{"} = -(i_A^{"} + i_B^{"}) \end{cases} \quad (9)$$

3.2Traction systems

Line-to-line voltages on the secondary windings for both Yd11 transformers are estimated utilizing voltage vectors shown in *Figure 4*, if the phase voltages of the primary windings are assumed to be equal [37].

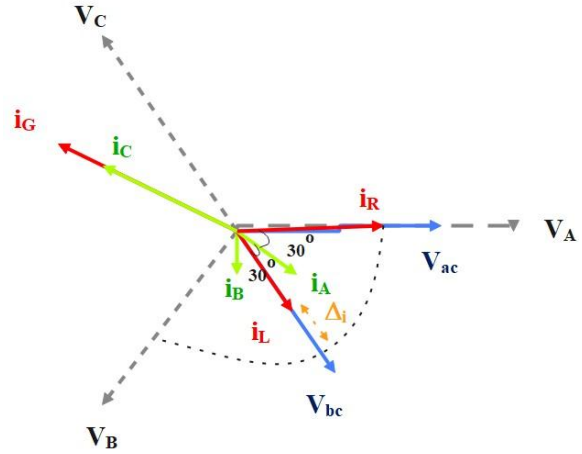

Figure 4 Primary and secondary vectors of Yd11 transformers

The voltage of five consecutive single phase (SP) is considered as Equation 10:

$$\begin{pmatrix} \dot{V}_1 \\ \dot{V}_2 \\ \dot{V}_3 \\ \dot{V}_4 \\ \dot{V}_5 \end{pmatrix} = \begin{pmatrix} \dot{V}_{ab_{Yd11}} - \dot{V}_{ba_{Yds}} \\ \dot{V}_{ca_{Yd5}} - \dot{V}_{ac_{Yd11}} \\ \dot{V}_{bc_{Yd11}} - \dot{V}_{cb_{Yds}} \\ \dot{V}_{ab_{Yds}} - \dot{V}_{ba_{Yd11}} \\ \dot{V}_{ca_{Yd11}} - \dot{V}_{ac_{Yd5}} \end{pmatrix} = \begin{pmatrix} 0 \\ 0 \\ 0 \\ 0 \\ 0 \end{pmatrix} \quad (10)$$

Consequently, the voltage over SPs is 0 due to this arrangement [38].

3.3Functionality of FBC

In terms of output voltage, the difference between the full bridge and the half-bridge is equal to the power supply voltage and one-half of it, respectively. This

argument suggests that a FBC is superior to a half-bridge converter. The full-bridge-based railway PQ compensator (FBRPQC), which has been proposed in this study, concurrently compensates for NSC, harmonics, and reactive power. A modified form of FLC, named the Type-2 FLC, is suggested for the current control approach.

The process FBC [39] has been separated into 6 phases and they are:
Phase $1(t_0 - t_1)$: Switches S1 and S4 are already on from the previous stage, the transformer is producing a negative output, and the performance rectifier is supplying electricity to the load at the start of this current stage. D1 and D4 Transformer voltages fall from VP to zero. When transformer current I_{Lr+} reaches to I_{Lr-}, this phase is complete.

Phase 2 $(t_1 - t_2)$: The switch is at t_1, and owing to the frequency of vibration being lower than the operating frequency, S1 is switched on in the ZVS condition. S1 is switched off in the ZCS status since S1 has been conducted. Transformer voltage rises from $VP-$ to 0 after this phase, and the primary transformer's I_{Lr+} reaches zero.

Phase 3 $(t_2 - t_3)$: As soon as S1 is off and S3 has finished the leading stage, S is switched on to create the ZCS state. Transformation current I_{Lr} rises from zero to I_{Lr+} as the voltage approaches $VP+$.

Phase $4(t_3 - t_4)$: While S3 and S4 are still functioning at this level, the transformer's voltage and current I_{Lr+} are both at zero.

Phase $5(t_4 - t_5)$: The transformer voltage rises to $VP+$ at the start of this stage, and I_{Lr} approaches I_{Lr+} as S1 is switched off under ZCS, S2 is turned on under ZVS, and S3 is still conducting from earlier stages. S2-S3-D2-D3 is used to transfer the output power.

Phase 6 $(t_5 - t_6)$: S4 is switched on under ZVS at the start of this stage, and S3 is turned off with ZCS procedure. In addition, I_{Lr} starts to fall from I_{Lr+} to zero when the transformer voltage decreases from $VP+$ to zero.

From$(t_6 - t_7)$, Phase 1 operation is repeated here.
The effectiveness of the converter is significantly increased compared to traditional resonant converters by a revolutionary zero voltage zero current switching technique (ZVZCS). An innovative strategy needs to be evaluated to reduce switch loss and prevent pressures on IGBTs caused by an abrupt rise in current via switches [40]. By using the ZVZCS switching mechanism, the losses in the turn-on/off switches are eliminated. *Figure 5* displays the FBC's switching pulses. *Figure 6* shows the topology of the FBC [41].

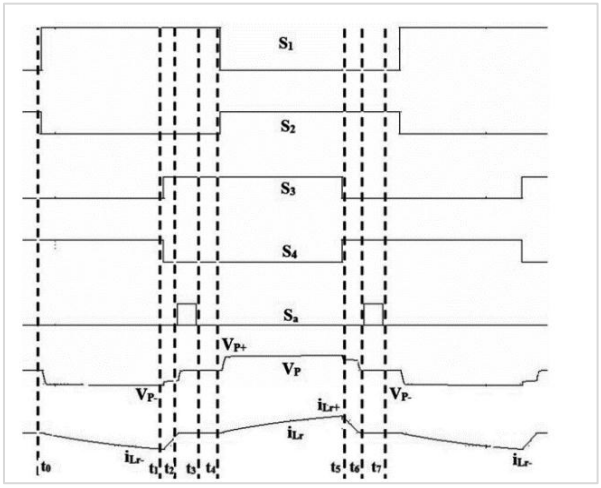

Figure 5 Switching pulses of FBC

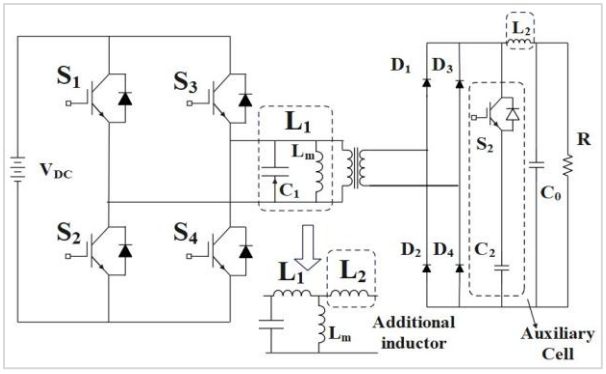

Figure 6 Topology of FBC

3.4Current control using Type-2 FLC

Type-2 FLC contains a foot point of uncertainty (FOU) that is declared as a tertiary measurement [42]. Here, $\tilde{A}$ is stated as the fuzzy set [43] in X and $\mu_A(x,u)$ is stated as membership function, which is mentioned in Equation 11.

$$\tilde{A} = \{((x,u), \mu_{\tilde{A}}(x,u)) | \forall x \in X\} \quad (11)$$

$\tilde{A}$ is stated in Equation 12.

$$\tilde{A} = \left\{ \int\int_{A} \mu_A(x,u)/(x,u) \right\} \quad (12)$$

Where $J_x \subseteq [0,1]$; $\iint$ () represents a combination of inclusive permissible x and u. For the universe of discourse, Φ is substituted as $\sum$. $\tilde{A}$ is modified as Equation 13, Equation 14 and Equation 15.

$$\tilde{A} = \left\{ \begin{matrix} (x, \mu(x)) | \forall \in X \\ A \end{matrix} \right\} \quad (13)$$

$$\tilde{A} = \int \left[\int f_x(u)/u \right]/x, J\tilde{A} = \int \left[\int f_x(u)/u \right]/x, J_x \subseteq [0,1] \quad (14)$$

If X and J_x are both discrete then

$$\tilde{A} = \sum_{i=1}^{n} \left[\sum f_{x_i}(u)/u \right] x_i \quad (15)$$

$\tilde{A}$ involves restricted area which requests FOU [44], [45]. The union of every chief affiliation is stated as Equation 16.

$$FOU(\tilde{A}) = \underset{x \in X}{UJ_x} \quad (16)$$

4.Results

Simulations executed in the MATLAB program (R2020b, version 9.9) are run to confirm the effectiveness of the suggested compensation and control technique. Because NSC correction underlies the capacity reduction, traction loads are modelled as resistive linear loads. *Table 1* displays the system and traction load simulation parameters. To demonstrate the viability of the suggested control technique, the system is independently simulated using both the conventional and suggested compensating methods. The MATLAB simulation model for the suggested design is depicted in *Figure 7.*

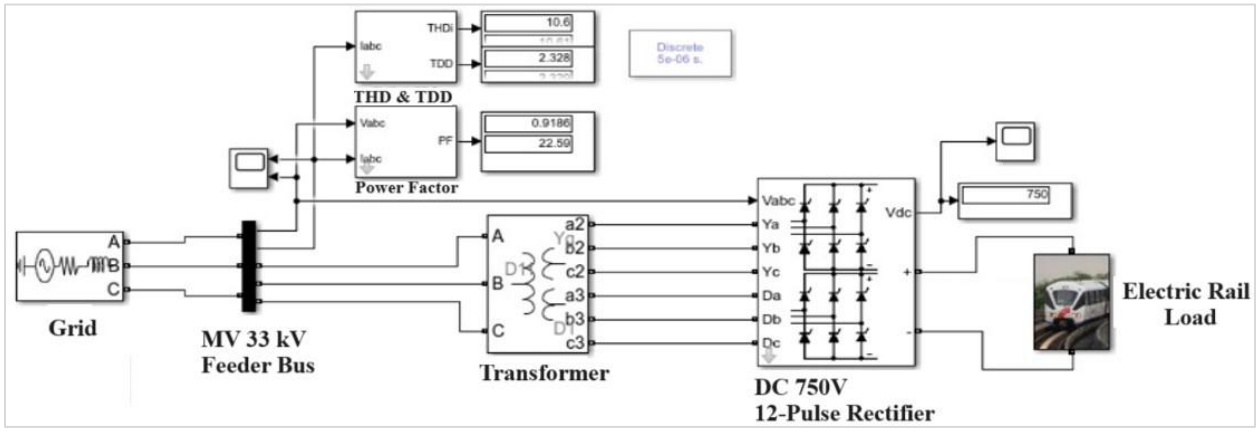

Figure 7 MATLAB simulink model for the proposed design

Table 1 Parameter specification

Parameter	Value
Transformers ratio (K_s)	28.4:2
Inductance (L_1)	0.5mH
TPS transformers ratio (K_T)	230:27.5
TPS ratio (K_T)	230:18.4
DC-link capacitors (C_1)	40 mF
Interface inductance (L_I)	0.5 mH
proportional gain (k_{p0})	2
DC-link capacitors (C_1, C_2)	40 mF
Proportional gain (k_p)	2
Initial integral gain (k_{i0})	0.2
Integral gain (k_i)	0.2
Hysteresis control (h)	2 A

As previously stated, the effectiveness of the suggested control method is unaffected by the type of TPS transformer. It also has no connection with the symmetrical Yd transformer's linear band. To demonstrate the viability of the suggested control mechanism, the projected structure is independently modelled for V/V, Yd11, and Scott transformers. Additionally, it is expected that traction loads fluctuate on both ends of TPS to evaluate the precision and reactivity of the recommended system. Analyses are thus completed in two steps. First, it is presumed that both parts of the TPS are trained at $\zeta = 0.5$. Secondly, it is assumed that TPS is analyzed at $\zeta = 0$. *Figure 8* shows the load currents of the Yd11 transformer. The FBRPQC reference currents for Yd11 are shown in *Figure 9.*

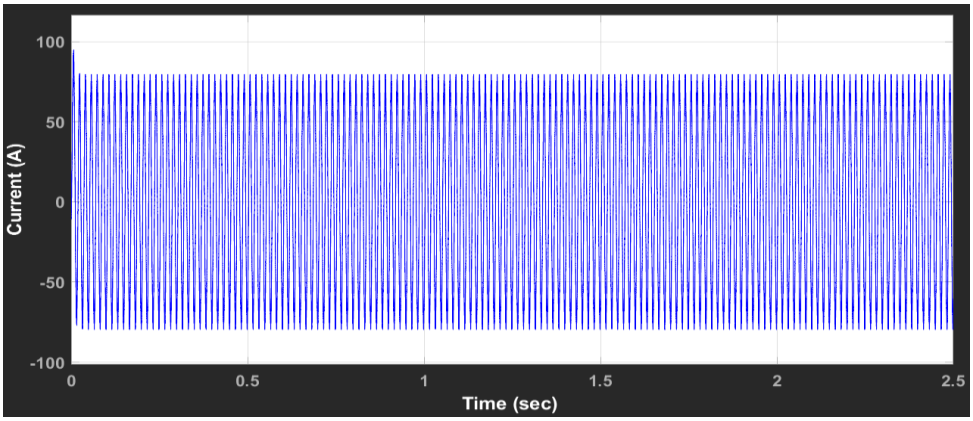

Figure 8 Load current

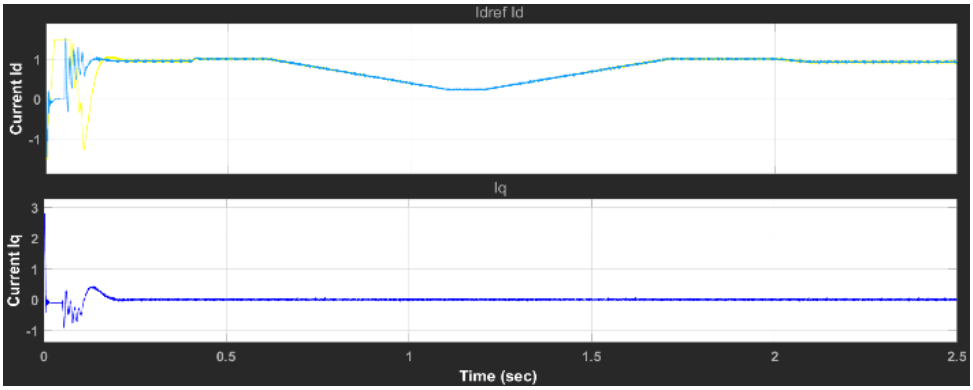

Figure 9 Reference current

5 MW and 2.5 MW are the traction load powers in feeders "a" and "c" respectively. At $t = 0.1s$, the FBRPQC is turned on, and compensation is initiated. Also, characteristics of traction load for feeder "a" are selected. For such load characteristics of feeder "c" these numbers are multiplied by two. The TPS is supposed to be unloaded ($\zeta = 0$) at time $t = 0.2s$. Each current control technique and the aforementioned transformer go through a separate simulation of this procedure. *Figure 10* shows the performance of DC link voltage. *Figure 11* shows the upper arm capacitor voltage and waveforms of voltage/current. In the *Figure 11(a)*, the upper arm capacitor voltages are displayed with respect to time. Similarly, *11(b*) displays the voltage and current values at the output side with respect to simulation running time. The lower frequency limit is the frequency at which the maximum permitted level of ripple voltage (specified by the design requirements) is exceeded. Applying the fundamental discharge for capacitors, it is calculated. Kilovolt amperes (kVA) or megavolt amperes (MVA) are the most common units used to express power transformer ratings. The primary and secondary windings are made to withstand the kVA or MVA values. Similarly, the positive and NSC are depicted in *Figure 12*.

The primary voltages of C1 and C2 are chosen to be 1200V and 1000 V, correspondingly, to produce a line voltage among the two capacitors to evaluate the DC-link control, whereby its voltage oscillations are demonstrated. The number of DC-link voltage is calculated at an unbalanced load ($\zeta = 0$) which is graphically represented in *Figure 10*. The power transfer formulation is equal to half of the complete traction load, resulting in a capacitance of 40 mF. As shown in *Figure 10*, the control method manages and maintains capacitor voltages by using FBRPQC at $t = 0.1s$. Slight voltage unbalance emerges at $t = 0.2s$ once the system load level fluctuates, and it is dampened after a regulation period, proving that the control approach is quick to react to continuous changes. *Figure 13* depicts the voltage and current of the Yd11 transformer. The Simulink findings for Scott and the V/V transformer are shown in *Tables 2* and *3*.

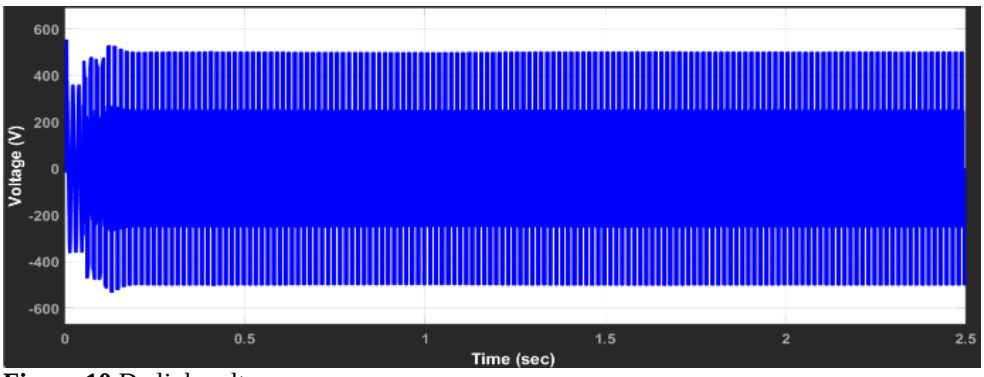

Figure 10 Dc link voltage

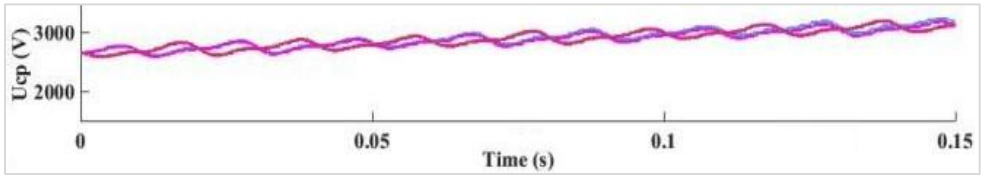

(a)

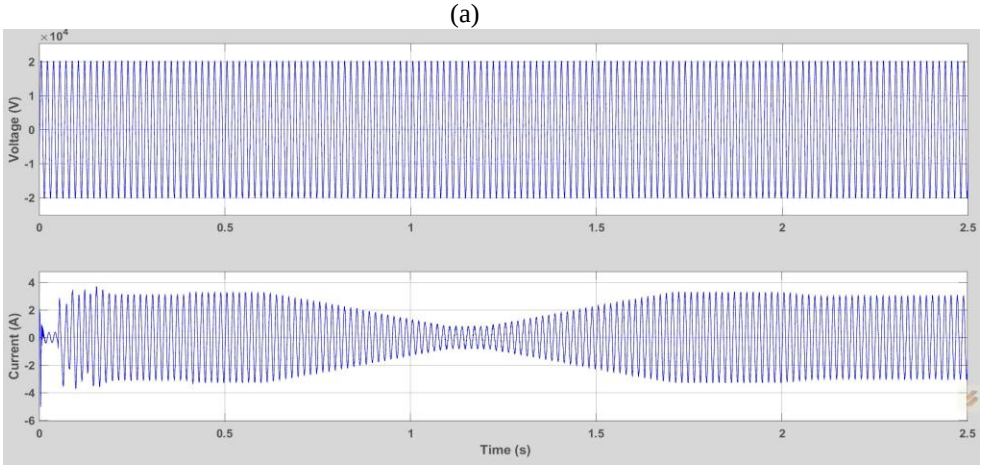

(b)

Figure 11 (a) Upper arm capacitor voltage (b) Waveform of output voltage and current

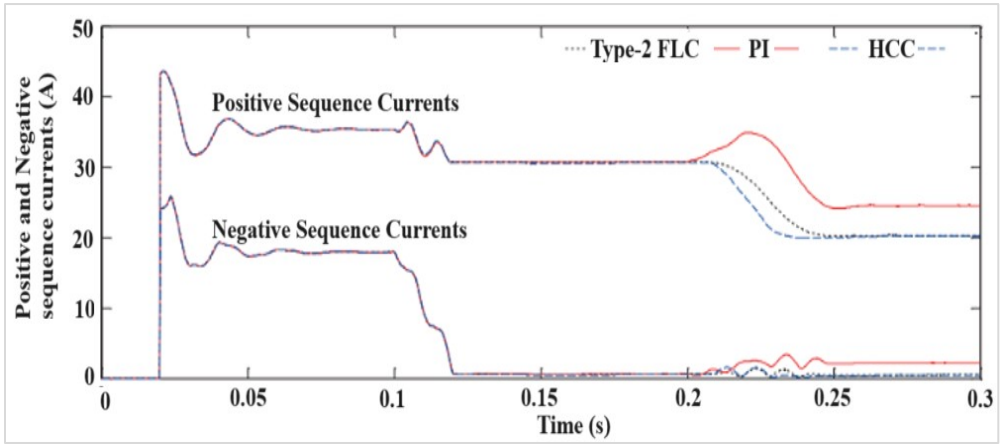

Figure 12 Positive and NSC

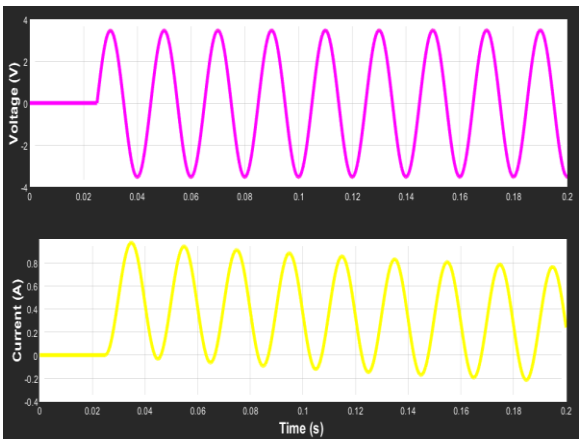

Figure 13 Voltage and Current of Yd11 Transformer

The system's $3-\varphi$ currents' total harmonic distortion (THD), which in some circumstances exceeded 39%, has been decreased to just 4%. On either side, traction loads take up a lot of reactive power, which results in a poor PF in the system. But as *Table 2* demonstrates, after correction, PF has increased from roughly 0.85 to 0.99. *Table 2* shows that whenever the suggested structure employs hysteresis current control (HCC), its static service is satisfactory but tracking error is present in its steady-state. THD of $3-\varphi$ currents in HCC are lower than the conventional approaches, and the HCC technique has a comparative advantage in harmonic correction. The steady-state effectiveness of the compensation scheme is enhanced when the PI modulation technique is used as opposed to the HCC technique. In other terms, PI has a lower imbalanced current ratio compared to the others. The typical PI technique, however, gives least performance in terms of reliability and flexibility. The imbalanced current ratio in the PI technique is higher when looking at current areas with the quantity of NSC. *Table 4* displays the Yd11 transformer's results. *Figures 14* and *15* show the performance of Yd11 transformer at $\varsigma = 0.5$ and $\varsigma = 0$, respectively. *Table 5* shows the comparative analysis of Yd11 transformer at $\varsigma = 0.5$ and $\varsigma = 0$, respectively with methods that are FLC, Type-1 FLC and proposed Type-2 FLC. Both the traditional FLC and type-1 FLC, struggle to model levels of uncertainty, whereas type-2 fuzzy logic systems (T2FLSs) are capable of achieving it. Compared to FLC and type-1 fuzzy sets, this additional dimension in type-2 provides additional degrees of freedom for an improved representation of uncertainty. Type-2 FLC has the proficiency to resolve undependability and exploitation of all applications. The results from *Table 5* demonstrate that Yd11 transformer produced better results of 1.71% and 1.64% distortion for existing FLC and Type-1 FLC respectively at $\varsigma = 0.5$. While considering the case at $\varsigma = 0$, it achieved distortion of 1.76% and 1.34% respectively in the existing FLC and Type-I FLC.

Table 2 Performance analysis of Scott transformer

Parameter constraints		**$\varsigma = 0.5$**			**$\varsigma = 0$**		
		After compensation			**After compensation**		
		HCC	**PI**	**Type-2 FLC**	**HCC**	**PI**	**Type-2 FLC**
THD% of source currents	A	2.19	2.25	2.39	3.18	3.52	3.02
	B	2.03	2.09	1.54	3.11	3.19	2.27
	C	1.62	1.78	1.48	2.52	2.93	2.21
PF		0.99	0.99	0.91	0.99	0.99	0.99

Table 3 Performance analysis of V/V transformer

Parameter constraints		**$\varsigma = 0.5$**			**$\varsigma = 0$**		
		After compensation			**After compensation**		
		HCC	**PI**	**Type-2 FLC**	**HCC**	**PI**	**Type-2 FLC**
THD% of source currents	A	3.46	2.39	2.24	1.99	2.97	1.83
	B	2.82	2.07	1.19	1.73	2.35	1.58
	C	2.13	1.92	1.57	1.68	2.15	1.17
PF		0.99	0.98	0.87	0.98	0.99	0.99

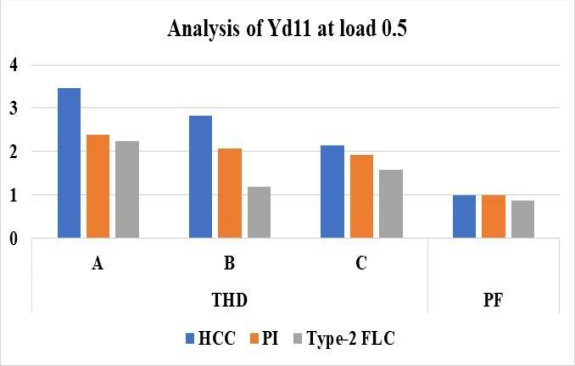

Figure 14 Analysis of Yd11 transformer at $\varsigma = 0.5$

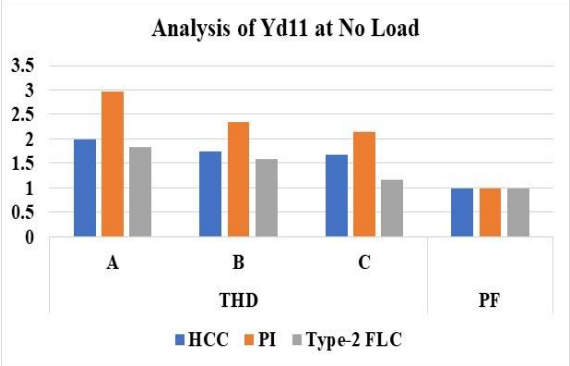

Figure 15 Analysis of Yd11 transformer at $\varsigma = 0$

Table 4 Performance analysis of Yd11 transformer

Parameter Constraints		$\varsigma = 0.5$			$\varsigma = 0$		
		After compensation			After compensation		
		HCC	PI	Type-2 FLC	HCC	PI	Type-2 FLC
THD% of source currents	A	2.13	2.75	1.34	2.55	2.95	1.72
	B	1.95	1.99	1.01	2.31	2.74	1.42
	C	1.62	1.67	1.57	2.03	2.48	1.17
PF		0.99	0.99	0.99	0.99	0.99	0.99

Table 5 Comparative analysis of Yd11 transformer

Parameter constraints		$\varsigma = 0.5$			$\varsigma = 0$		
		After compensation			After compensation		
		FLC	Type-1 FLC	Type-2 FLC	FLC	Type-2 FLC	Type-2 FLC
THD% of source currents	A	1.91	1.56	1.34	2.16	1.87	1.72
	B	1.64	1.37	1.01	1.89	1.62	1.42
	C	1.71	1.64	1.58	1.76	1.34	1.16
PF		0.99	0.99	0.99	0.99	0.99	0.99

5.Discussion

In this article, the performance of the Yd11 transformer is examined in a TPS, and its superiority over the Scott and V/V transformers is demonstrated. In the comparative analysis, the Yd11 transformer is compared with existing FLC and Type-1 FLC. An evaluation and analysis are carried out in accordance with the system connectivity, factors affecting PQ, and economic considerations. In the analysis, under both balanced and unbalanced conditions, RPQC serves as the primary compensator and TPS as the auxiliary compensator. Due to the quick and dynamic nature of the traction loads, the suggested control system uses a PI controller based on a Type-2 FLC. Carrier-based PWM signals and output control variables are combined to produce the pulse signals for Full Bridge RPQC switches. The results of the simulations for the Yd11, V/V, and Scott transformers show the effectiveness of the proposed control technique. The results emphatically demonstrate that at loads of $\varsigma = 0.5$ and $\varsigma = 0$ respectively, the Yd11 transformer produced better results of 1.57% and 1.17% distortion, as well as PF of 0.99 which is superior to other transformers. The comparative analysis at $\varsigma = 0.5$, for existing FLC and Type-1 FLC, respectively, with Yd11 transformer shows the results of 1.71% and 1.64% distortion. The conventional FLC and Type-I FLC attained distortions of 1.76% and 1.34%, respectively, while evaluating the case at $\varsigma = 0$.

Limitations

Losses and noise are considerable when employing the FBC which requires more switching components and resembles a half-bridge inverter. The section that connects the ground point to the load, however, is an extra segment. Four switches are used in a full bridge circuit. This has the advantage of dispersing the stress among them, which is advantageous at high power but useless at low power. However, 4 switches will cost you more. Two 'high side' drives, which refer to isolated or level-shifted gate drive signals, are required for a full bridge. Bridge circuits, as opposed to push-pull or single-ended forward, which require

far greater voltage ratings for switches, limit the switch voltage stress to the input voltage maximum. The configuration of the fuzzy controller, namely the type of fuzzy AND operator used, affects the difficulties involved with analytical-structure derivation. This is factual for type-2 fuzzy controllers, but it is much harder to implement a fuzzy controller that uses the other operator. Type-2 FLCs are more sophisticated structurally than type-1 FLCs because they have more parts (such as type reducers), additional parameters (such as an uncertainty footprint in type-2 fuzzy sets), and a more complicated inference method. A complete list of abbreviations is shown in *Appendix I.*

6.Conclusion and future work

Currently, the proliferation of electrical railway systems has led to several PQ issues. This study focuses on a specific type of full-bridge-based RPQC device that effectively addresses NSC, distortions, and reactive power simultaneously. To ensure the effectiveness of the FBRPQC across various types of transformers used in the traction system, an enhanced multifunctional control technique is proposed. The current control system employs a PI controller-based Type-2 FLC due to the rapid and dynamic nature of traction loads. Pulse signals for the FBRPQC switches are generated by integrating output control variables with PWM techniques. The utility of this control approach is demonstrated through simulations for Yd11 transformers. This study explores a specific type of traction transformer, and its power performance is analyzed. Furthermore, THD is assessed through FFT analysis for multiple transformers. Notably, the Yd11-based transformer exhibits the lowest THD levels, measuring 1.57 at ς=0.5 and 1.17 at ς=0, respectively. Voltage imbalances occur when the active compensator is disconnected, prompting an analysis of the co-phase system both with and without the device. The introduction of the active power compensator successfully resolves voltage imbalances. In the future, the enhancement of PQ in railway traction systems will benefit from novel hybrid rule-based techniques designed to improve system efficiency.

Acknowledgment

None.

Conflicts of interest

The authors have no conflicts of interest to declare.

Author's contribution statement

Deepak Kumar Goyal: Conceptualization, investigation, methodology, dataset collection, implementation, result analysis and comparison, writing – original draft, Writing – review and editing. **Dinesh Birla:** Project administration, supervision, investigation on challenges and manuscript preparation.

References

[1] Letizia PS, Signorino D, Crotti G. Impact of DC transient disturbances on harmonic performance of voltage transformers for AC railway applications. Sensors. 2022; 22(6):1-12.

[2] Liu L, Dai N, Lao KW, Hua W. A co-phase traction power supply system based on asymmetric three-leg hybrid power quality conditioner. IEEE Transactions on Vehicular Technology. 2020; 69(12):14645-56.

[3] Zhao L, Wu M, Liu Q, Peng P, Li J. Hybrid power quality compensation system for electric railway supplied by the hypotenuse of a Scott transformer. IEEE Access. 2020; 8:227024-35.

[4] Thentral TM, Palanisamy R, Usha S, Vishnuram P, Bajaj M, Sharma NK, et al. The improved unified power quality conditioner with the modular multilevel converter for power quality improvement. International Transactions on Electrical Energy Systems. 2022; 2022:1-15.

[5] Olives-camps JC, Mauricio JM, Maza-ortega JM, Gómez-expósito A. Distributed consensus-based secondary control of multi-terminal DC railway systems. International Journal of Electrical Power & Energy Systems. 2023; 148:108986.

[6] Feng C, Gao Z, Sun Y, Chen P. Electric railway smart microgrid system with integration of multiple energy systems and power-quality improvement. Electric Power Systems Research. 2021; 199:107459.

[7] Kebede AB, Worku GB. Power electronics converter application in traction power supply system. American Journal of Electrical Power and Energy Systems. 2020; 9(4):67-73.

[8] Huang X, Liao Q, Li Q, Tang S, Sun K. Power management in co-phase traction power supply system with super capacitor energy storage for electrified railways. Railway Engineering Science. 2020; 28:85-96.

[9] Malik M, Dahiya R. Optimization of dc-dc converters for off-grid lighting in trains using artificial neural networks. In intelligent communication, control and devices: proceedings of ICICCD 2018 2020 (pp. 333-44). Springer Singapore.

[10] Sun P, Li K, Li Y, Zhang L. DC voltage control for MMC-based railway power supply integrated with renewable generation. IET Renewable Power Generation. 2020; 14(18):3679-89.

[11] Morais VA, Martins AP. Traction power substation balance and losses estimation in AC railways using a power transfer device through Monte Carlo analysis. Railway Engineering Science. 2022; 30(1):71-95.

[12] Cheng P, Kong H, Ma J, Jia L. Overview of resilient traction power supply systems in railways with interconnected microgrid. CSEE Journal of Power and Energy Systems. 2020; 7(5):1122-32.

[13] Li Y, Li K, Zhang L, Li Y. Novel double-layer DC/AC railway traction power supply system with renewable integration. IET Renewable Power Generation. 2020; 14(18):3616-27.
[14] Wang L, Pang Y, Wong MC, Xu Q, Zhou X, He Z. A new topology of three-port power hub converter with power quality compensation for remote area residential power supply. IEEE Transactions on Industrial Electronics. 2020; 68(11):10336-48.
[15] Tasiu IA, Liu Z, Wu S, Yu W, Al-barashi M, Ojo JO. Review of recent control strategies for the traction converters in high-speed train. IEEE Transactions on Transportation Electrification. 2022; 8(2):2311-33.
[16] Arabahmadi M, Banejad M, Dastfan A. Hybrid compensation method for traction power quality compensators in electrified railway power supply system. Global Energy Interconnection. 2021; 4(2):158-68.
[17] Amira CR, Ramdane B, Hamza B, Meriem A, Imen M. Genetic algorithm approach of HB-RPC for adaptive power quality improvement in railway traction Chain. In international conference on electrical, communication, and computer engineering 2021 (pp. 1-6). IEEE.
[18] Goyal DK, Birla D. The various traction transformers and power quality improvement using YD traction transformer in electrical railway traction system. Journal of Active & Passive Electronic Devices. 2021; 16(2):131-40.
[19] Lei M, Zhao C, Li Z, He J. Circuit dynamics analysis and control of the full-bridge five-branch modular multilevel converter for comprehensive power quality management of cophase railway power system. IEEE Transactions on Industrial Electronics. 2021; 69(4):3278-91.
[20] Lei M, Wang Y, Zhao C. Optimized operation of the full-bridge five-branch modular multilevel converter for power quality enhancement of cophase railway power system. IEEE Transactions on Transportation Electrification. 2021; 8(1):590-604.
[21] Li T, Shi Y. Power quality management strategy for high-speed railway traction power supply system based on MMC-RPC. Energies. 2022; 15(14):1-20.
[22] Wang Y, Xin Y, Xie Z, Mu X, Chen X. Research on low-frequency stability under emergency power supply scheme of photovoltaic and battery access railway traction power supply system. Energies. 2023; 16(12):1-32.
[23] Li T, Shi Y. Application of MMC-RPC in High-speed railway traction power supply system based on energy storage. Applied Sciences. 2022; 12(19):1-19.
[24] Lai J, Chen M, Dai X, Zhao N. Energy management strategy adopting power transfer device considering power quality improvement and regenerative braking energy utilization for double-modes traction system. CPSS Transactions on Power Electronics and Applications. 2022; 7(1):103-11.
[25] Tang M, Zhou Y, Liang K, Liu X, Tong X. Cophase traction power supply system based-MMC-Vv wiring. IEEE Access. 2022; 10:96016-25.
[26] Suslov K, Kryukov A, Voronina E, Fesak I. Modeling power flows and electromagnetic fields induced by compact overhead lines feeding traction substations of mainline railroads. Applied Sciences. 2023; 13(7):1-21.
[27] Suslov K, Kryukov A, Ilyushin P, Kryukov A, Shepovalova O. Modeling of modes of traction power supply systems equipped with renewable energy sources. Energy Reports. 2023; 9:447-61.
[28] Kampczyk A, Rombalska K. Configuration of the geometric state of railway tracks in the sustainability development of electrified traction systems. Sensors. 2023; 23(5):1-33.
[29] Fedele E, Iannuzzi D, Tricoli P, Del PA. NPC-based multi-source inverters for multimode DC rail traction systems. IEEE Transactions on Transportation Electrification. 2022; 9(1):1289-99.
[30] Riabov I, Goolak S, Kondratieva L, Overianova L. Increasing the energy efficiency of the multi-motor traction electric drive of an electric locomotive for railway quarry transport. Engineering Science and Technology, an International Journal. 2023; 42:1-10.
[31] Kapoor T, Wang H, Núñez A, Dollevoet R. Predicting traction return current in electric railway systems through physics-informed neural networks. In symposium series on computational intelligence 2022 (pp. 1460-8). IEEE.
[32] Fazel SS, Jafari KH, Madadi KH. An efficient strategy for power rating reduction of back-to-back converters used in railway power conditioner. International Journal of Railway Research. 2016; 3(1):19-28.
[33] Kaleybar HJ, Kojabadi HM, Fallah M, Fazel SS, Chang L. Impacts of traction transformers on power rating of railway power quality compensator. In IEEE 8th international power electronics and motion control conference (IPEMC-ECCE Asia) 2016 (pp. 2229-36). IEEE.
[34] Kaleybar HJ, Farshad S. A comprehensive control strategy of railway power quality compensator for AC traction power supply systems. Turkish Journal of Electrical Engineering and Computer Sciences. 2016; 24(6):4582-603.
[35] Kaleybar HJ, Kazemzadeh R, Fazel SS. A comprehensive study on performance of YD transformer in AC electrified railway systems. Journal of Electrical Engineering. 2016; 16(2).
[36] Setiabudy R, Surya I, Herlina H. Phase-shifting method with Dy11 transformer to reduce harmonics. In international conference on electrical engineering and computer science 2019 (pp. 416-21). IEEE.
[37] Paul D, Goswami AK, Kumar S, Jain S, Pandey A. Propagation of voltage sag considering different winding connections: Impact on the healthiness of transformers. IEEE Transactions on Industry Applications. 2020; 56(6):6186-96.
[38] Ye H, Cao W, Chen W, Wu H, He G, Li G, et al. An AC fault ride through method for MMC-HVDC system in offshore applications including DC current-limiting inductors. IEEE Transactions on Power Delivery. 2021; 37(4):2818-30.

[39] Vijayakumar A, Stonier AA, Peter G, Loganathan AK, Ganji V. Power quality enhancement in asymmetrical cascaded multilevel inverter using modified carrier level shifted pulse width modulation approach. IET Power Electronics. 2022:1-13
[40] Oluwasogo ES, Cha H. A quadratic quasi-z-source full-bridge isolated DC–DC converter with high reliability for wide input applications. IEEE Transactions on Industrial Electronics. 2022; 69(10):10090-100.
[41] Tai YK, Hwu KI. A novel ZVS/ZCS push-pull LC resonant DC-DC converter for energy sources. Energies. 2023; 16(6):2892.
[42] Soliman AM, Eldin MB, Mehanna MA. Application of WOA tuned type-2 FLC for LFC of two area power system with RFB and solar park considering TCPS in interline. IEEE Access. 2022; 10:112007-18.
[43] Qin S, Zhang C, Zhao T, Tong W, Bao Q, Mao Y. Dynamic high-type interval type-2 fuzzy logic control for photoelectric tracking system. Processes. 2022; 10(3):1-21.
[44] Arifin B, Suprapto BY, Prasetyowati SA, Nawawi Z. Steering control in electric power steering autonomous vehicle using type-2 fuzzy logic control and PI control. World Electric Vehicle Journal. 2022; 13(3):1-21.
[45] Sharma R, Kumar A. Optimal Interval type-2 fuzzy logic control based closed-loop regulation of mean arterial blood pressure using the controlled drug administration. IEEE Sensors Journal. 2022; 22(7):7195-207.

Deepak Kumar Goyal received the B.E. degree in Electrical Engineering from MBM Engineering college, Jodhpur, Rajasthan and M.Tech. degree in Power Apparatus & Electric Drives from IIT Roorkee, Uttarakhand, India in 2002 and 2005 respectively. He is presently pursuing his doctorate studies from Rajasthan Technical University, Kota, Rajasthan in the field of Power Electronics and Drives. His main research interest includes power quality issues, Electric Drive, traction system. He is presently employed in Government Engineering College Bharatpur, Rajasthan as Assistant Professor in Department of Electrical Engineering. He has over 17 years of teaching experience.
Email: dkg_elect@rediffmail.com

Dinesh Birla received the P.hD. from IIT Roorkee, Uttarakhand, India and his main research interest includes Power System, Power Electronics, Optimization. He is Professor in the Department of Electrical Engineering at the Rajasthan Technical University, Kota, Rajasthan, India. He has authored many books and research papers in Power System Protection, Power Electronics & Renewable Energy. He has been on the editorial board and reviewer of many journals. He also served on many program committees and conducted conferences and workshops in the area. He is a Life Member ISTE, Member IE (India), Life Member of Solar Energy Society of India, Member IEANG and Life Member of Society of EMC Engineers.
Email: dbirla@rtu.ac.in

Appendix I

S. No.	Abbreviation	Description
1	AC-AC	Alternating Current-Alternating Current
2	AC-DC	Alternating current-Direct Current
3	CC	Current Compensation
4	COHL	Compacted Over Headed Lined
5	DFC	Differential Flatness Control
6	DG	Distributed Generation
7	EMI	Electro-Magnetic Interference
8	ERPS	Electric Railway Power System
9	ES	Energy Storage
10	ERS	Electrified Railway System
11	FB5B - MMC	Full-Bridge Five-Branch Modular Multilevel Converter
12	FBC	Full Bridge Converter
13	FBRPQC	Full-Bridge-Based Railway Power Quality Compensator
14	FLC	Fuzzy Logic Control
15	FOU	Foot point of Uncertainty
16	GA	Genetic Algorithm
17	HB-RPC	Half-Bridge-converter-based RPC
18	HCC	Hysteresis Current Control
19	IGBT	Insulated Gate Bipolar Transistor
20	KVA	Kilo-Volt Amperes
21	MMC-RPC	Modular Multilevel Converter Type Railway Power Conditioner
22	MSI	Multi-Source Inverters
23	MVA	Megavolt Amperes
24	NPC	Neutral Point Clamped
25	NSC	Negative Sequence Current
26	PE	Power Electronics
27	PF	Power Factor
28	PI	Proportional Integral
29	PQ	Power Quality
30	PV	Photo-Voltaic
31	PWM	Pulse Width Modulation
32	RPC	Railway Power Conditioner
33	RPQC	Railway Power Quality Compensator
34	RPSS	Railway Power Supply System
35	SC	Super-Capacitor
36	SP	Single Phase
37	SVC	Static Volt Ampere Reactive Compensator
38	THD	Total Harmonic Distortion
39	TPS	Traction Power Substation
40	Type-2 FLC	Type-2 Fuzzy Logic Controller
41	VAR	Volt-Ampere Reactive
42	VSC	Voltage Source Converter
43	VSG	Virtual Synchronous Generator
44	ZCS	Zero Current Switching
45	ZVS	Zero Voltage Switching
46	ZVZCS	Zero Voltage Zero Current Switching